13th International Conference on Applications of Statistics and Probability in Civil Engineering, ICASP13
Seoul, South Korea, May 26-30, 2019

Simulation of Fluctuating Wind Speed Fields by Stochastic Harmonic Function Representation Method Based on Joint Wavenumber-Frequency Power Spectrum

Yupeng Song
Ph.D. student, College of Civil Engineering, Tongji University, Shanghai, China

Jianbing Chen
Professor, College of Civil Engineering & State Key Laboratory of Disaster Reduction in Civil Engineering, Tongji University, Shanghai, China

Yongbo Peng
Professor, State Key Laboratory of Disaster Reduction in Civil Engineering, Tongji University, Shanghai, China；Shanghai Institute of Disaster Prevention and Relief, Tongji University, Shanghai, China

Jie Li
Professor, College of Civil Engineering & State Key Laboratory of Disaster Reduction in Civil Engineering, Tongji University, Shanghai, China

ABSTRACT: Simulation of wind speed fields usually plays a crucial role in the reliability analysis of large-size and high-rise structures such as tall buildings, long-span bridges and offshore wind turbines. To simulate a fluctuating wind speed field by the spectral representation method (SRM), two schemes can be adopted: (1) the conventional SRM, involving the decomposition of the cross power spectrum density (XPSD) matrix of fluctuating wind speed inevitably; and (2) the joint wavenumber-frequency spectrum based SRM, where a series of trigonometric functions are directly superimposed without any decompositions of XPSD matrix. However, both the two approaches involve large amounts of random variables, which hinder the reliability analysis of structures. In this paper, the stochastic harmonic function (SHF) representation method is extended and integrated with the joint wavenumber-frequency power spectrum to simulate fluctuating wind speed fields in one spatial dimension. Further, an efficient non-uniformly discretized scheme in wavenumber and frequency directions is suggested such that the number of random variables is dramatically reduced. Simulation results demonstrate the efficiency and validity of the proposed method.

Simulation of fluctuating wind speed field is of paramount significance in the design of wind sensitive structures such as long-span bridges, tall buildings and megawatt wind turbines (Zeng et al. 2017). Unlike the complexity in the physical mechanism based models such as the computational fluid dynamics (CFD) method (Huang et al. 2018), the fluctuating wind speed field can be modeled as a random vector process or a random field in a simple mathematical manner for engineering applications (Shinozuka 1971). The spectral representation method (SRM), as the most widely used method, has been investigated and applied in structural wind engineering over decades (Tao et al. 2018). However, to simulate the fluctuating wind field as a random vector process with the SRM, decompositions of the cross power spectrum density (PSD) matrix are needed at each discretized frequency, which suffers from poor

efficiency in simulation of large scale wind speed fields (Tao et al. 2018). To circumvent the decompositions of matrix, a wavenumber-frequency joint spectrum based SRM has been developed in recent years (Benowitz & Deodatis 2015; Peng et al. 2017; Chen et al. 2018a; Song et al. 2018a). In this method, the fluctuating wind speed field is modeled as a temporal-spatial random field by straightforward superposition of trigonometric series, which is of much convenience in practice.

In spite of the advances in wind field simulation, a large number of random variables (phase angles) are usually involved in these methods, which hinders the reliability analysis of structures (Spanos et al. 2007). Although several approaches have been investigated to reduce the number of random variables (Li et al. 2012; Liu et al. 2018), it remains an open problem. The stochastic harmonic function (SHF) representation method, which regards both the phase angles and discretized frequencies (wavenumbers) as random variables, can reproduce the target PSD exactly no matter how many trigonometric components are retained (Chen et al. 2013; 2017; 2018b). Therefore, it provides a promising approach in reducing the number of random variables for wind field simulation.

In the present paper, the SHF representation will be extended to two-dimensional (2D) nonhomogeneous random field case and then integrated with the wavenumber-frequency joint spectrum to simulate fluctuating wind fields in one spatial dimension. The present paper is organized as follows. Section 1 briefly introduces the wavenumber-frequency joint spectrum for nonhomogeneous fluctuating wind fields in one spatial dimension and its spectral representation. In Section 2, the SHF representation for 2D homogeneous random field is firstly revisited, and then is extended to nonhomogeneous case. In Section 3, a numerical example for simulation of fluctuating wind speed field for a wind turbine tower is carried out to demonstrate the effectiveness of the proposed method. Concluding remarks pertaining to this study are provided in Section 4.

1. WIND FIELD SIMULATION BY THE JOINT SPECTRUM BASED SRM

The joint spectrum based SRM was firstly proposed by Shinozuka (1971). However, it has not been well noticed for decades until Benowitz and Deodatis (2015) simulated one-spatial dimensional homogeneous wind speed field along this line. It was then quickly extended to one-spatial dimensional nonhomogeneous and nonstationary cases (Peng et al. 2017) and two-spatial dimensional homogeneous and nonhomogeneous cases (Chen et al. 2018a; Song et al. 2018a). In the present paper, only the one-spatial nonhomogeneous case is considered.

1.1. Joint spectrum for nonhomogeneous fluctuating wind speed fields in one-spatial dimension

For clarity, the fluctuating wind speed filed in one-spatial dimension is denoted by $u(z,t)$, in which z axes denotes the vertical spatial direction and t is the time. One can easily observe that $u(z,t)$ is essentially a 2D temporal-spatial random field.

The Kaimal spectrum and the one-spatial dimensional Davenport coherence model are employed (Peng et al. 2017; Song et al. 2018b), i.e.,

$$S^{\mathrm{Kai}}(\omega)=\frac{50zu_*^2}{\pi U(z)\left(1+\frac{50}{2\pi U(z)}\omega z\right)^{5/3}} \tag{1}$$

$$\begin{aligned}\rho(\xi,\omega)&=\exp\left(-\frac{C_z}{2\pi U_{10}}|\omega|\cdot|z_1-z_2|\right)\\&=\exp\left(-\frac{C_z}{2\pi U_{10}}|\omega|\cdot|\xi|\right)\end{aligned} \tag{2}$$

where $S^{\mathrm{Kai}}(\omega)$ denotes the Kaimal spectrum, ω is the circular frequency, and u_* is the shear velocity. $\rho(\xi,\omega)$ denotes the coherence function, C_z is the exponential decay coefficient, U_{10} is the mean wind speed at 10m high, and

$\xi = z_1 - z_2$ is the spatial separation. $U(z)$ denotes the mean wind speed at the height z and follows the following logarithmic law,

$$U(z) = \frac{u_*}{\kappa} \ln \frac{z}{z_0} \tag{3}$$

in which κ is the von Karman constant and z_0 is the roughness.

Then, the joint wavenumber-frequency spectrum of the random field can be derived as (Peng et al. 2017; Song et al. 2018b)

$$\begin{aligned} S(z,k,\omega) &= S^{\mathrm{Kai}}(\omega)\rho(\omega,k) \\ &= S^{\mathrm{Kai}}(\omega)\frac{C_z}{2\pi^2 U_{10}} \frac{|\omega|}{\left(\frac{C_z}{2\pi U_{10}}\right)^2 \omega^2 + k^2} \end{aligned} \tag{4}$$

where $S(z,k,\omega)$ denotes the joint spectrum in wavenumber-frequency domain, k is the wavenumber in z direction, and $\rho(\omega,k)$ is the Fourier transform of $\rho(\xi,\omega)$ with respect to ξ.

It is noted that the wind spectrum and the coherence model can also take other forms.

1.2. Spectral representation for wind speed fields

Once the spectrum is obtained for the random field, the SRM is readily to be employed to generate fluctuating wind speed field samples (Peng et al. 2017; Song et al. 2018b), i.e.

$$\begin{aligned} u(z,t) = \sum_{i=1}^{N_k}\sum_{j=1}^{N_\omega} \sqrt{4S(z,k_i,\omega_j)\Delta k \Delta\omega} \times \\ [\cos(k_i z + \omega_j t + \phi_{ij}^{(1)}) + \cos(k_i z - \omega_j t + \phi_{ij}^{(2)})] \end{aligned} \tag{5}$$

where k_i 's are the discretized wavenumbers, $k_i = i\Delta k, i = 1,2,\cdots,N_k$, $\Delta k = k^{\mathrm{U}}/N_k$, k^{U} is the upper cut-off wavenumber, and N_k is the number of discretized wavenumbers. Likewise, ω_j 's are the discretized circular frequencies, $\omega_j = j\Delta k$, $j = 1,2,\cdots,N_\omega$, $\Delta\omega = \omega^{\mathrm{U}}/N_\omega$, ω^{U} is the upper cut-off frequency, and N_ω is the number of discretized frequencies. $\phi_{ij}^{(1)}$'s and $\phi_{ij}^{(2)}$'s are two different sets of independent random phase angles uniformly distributed over $[0, 2\pi]$.

Eq.(5) indicates that based on the joint spectrum the wind speed field can be simulated by summing the trigonometric functions directly. This circumvents the decomposition of the XPSD matrix involved in the conventional methods (Tao et al. 2018). However, it is worth noting that Eq.(5) is a two-fold summation over the wavenumber-frequency domain. To obtain a satisfactory simulation result, the numbers N_k and N_w are usually of the order of magnitude $\mathcal{O}(10^3)$. Therefore, the total number of terms involved in Eq.(5) is in the order of magnitude $\mathcal{O}(10^5) \sim \mathcal{O}(10^6)$. A large number of random phase angles are involved simultaneously. Although the fast Fourier transform (FFT) technique can be employed in place of the summation to improve simulation efficiency, it has nothing to do with reducing the number of random phase angles. In the present paper, the SHF representation is adopted, through which the computational efforts as well as the number of random variables can be dramatically reduced.

2. STOCHASTIC HARMONIC FUNCTION REPRESENTATION FOR WIND SPEED FIELDS

The SHF representation was proposed by Chen et al. (2013) for 1D stationary random process. It was later extended to 1D nonstationary random process (Chen et al. 2017) and 2D homogeneous random field (Chen et al. 2018b). In the present paper, the SHF representation is further extended to 2D nonhomogeneous cases to simulate one-spatial dimensional nonhomogeneous fluctuating wind speed fields. To make it clear, the basic idea of the SHF representation for 2D homogeneous random field is firstly revisited.

2.1. SHF representation for 2D homogeneous random fields

In the SHF representation, both phase angles and discretized frequencies (wavenumbers) are taken

as random variables. In contrast, only the phase angles are random variables in the SRM.

For clarity, the spectrum of the 2D homogeneous random field $Y(x_1,x_2)$ is denoted by $S_Y(k_1,k_2)$. The wavenumber domain of interest is $D_0=[0,k_1^{\mathrm{U}}]\times[0,k_2^{\mathrm{U}}]$, where k_1^{U} and k_2^{U} are the upper cut-off wavenumbers in x_1 and x_2 directions, respectively. Partition $[0,k_1^{\mathrm{U}}]$ into a set of non-overlapping subintervals $[\underline{k}_i^{(1)},\overline{k}_i^{(1)}]$ $(i=1,2,...,N_1)$ such that $[0,k_1^{\mathrm{U}}]=\cup_{i=1}^{N_1}[\underline{k}_i^{(1)},\overline{k}_i^{(1)}]$ and $[\underline{k}_i^{(1)},\overline{k}_i^{(1)}]\cap[\underline{k}_l^{(1)},\overline{k}_l^{(1)}]=\varnothing$, $\forall i\neq l$. Likewise, partition $[0,k_2^{\mathrm{U}}]$ into $[\underline{k}_j^{(2)},\overline{k}_j^{(2)}]$ $(j=1,2,...,N_2)$.

Thus, the SHF representation for the 2D homogeneous random field can be expressed as

$$Y(x_1,x_2)=\sum_{i=1}^{N_1}\sum_{j=1}^{N_2}A(K_i^{(1)},K_j^{(2)})\times[\cos(K_i^{(1)}x_1+K_j^{(2)}x_2+\phi_{ij}^{(1)})+\cos(K_i^{(1)}x_1-K_j^{(2)}x_2+\phi_{ij}^{(2)})] \quad (6)$$

where $(K_i^{(1)},K_j^{(2)})$ is a random vector of wavenumber in the subdomain $D_{ij}=[\underline{k}_i^{(1)},\overline{k}_i^{(1)}]\times[\underline{k}_j^{(2)},\overline{k}_j^{(2)}]$ with the probability density function (PDF) $p_{K_i^{(1)},K_j^{(2)}}(k_1,k_2)$. $\phi_{ij}^{(1)}$'s and $\phi_{ij}^{(2)}$'s are uniform random phases independently distributed over [0, 2π].

For convenience, $(K_i^{(1)},K_j^{(2)})$ is taken as a uniformly distributed random vector over D_{ij}, i.e., the PDF of $(K_i^{(1)},K_j^{(2)})$ is

$$p_{K_i^{(1)},K_j^{(2)}}(k_1,k_2)=\frac{1}{(\overline{k}_i^{(1)}-\underline{k}_i^{(1)})(\overline{k}_j^{(2)}-\underline{k}_j^{(2)})} \quad (7)$$

Then, the amplitudes are given by

$$A(K_i^{(1)},K_j^{(2)})=\sqrt{4S_Y(K_i^{(1)},K_j^{(2)})(\overline{k}_i^{(1)}-\underline{k}_i^{(1)})(\overline{k}_j^{(2)}-\underline{k}_j^{(2)})} \quad (8)$$

Obviously, the SHF representation is an extension of the SRM. Besides, one can easily prove that the PSD of $Y(x_1,x_2)$ represented by Eq.(6) is identical to $S_Y(k_1,k_2)$ no matter how many harmonic components are retained in Eq.(6). Therefore, the number of random variables can be markedly reduced.

2.2. Extension of the SHF representation for 2D nonhomogeneous random fields

The concerned 2D random field in this study $u(z,t)$ is nonhomogeneous in spatial dimension and stationary in temporal dimension. This is due to the fact that its spectrum $S(z,k,\omega)$ is only dependent on the spatial position but not on the time.

Similar to the 2D homogeneous case, the wavenumber-frequency domain of interest is denoted by $D_0=[0,k^{\mathrm{U}}]\times[0,\omega^{\mathrm{U}}]$, where k^{U} and ω^{U} are the upper cut-off wavenumber and frequency, respectively. Partition $[0,k^{\mathrm{U}}]$ into a set of non-overlapping subintervals $[\underline{k}_i,\overline{k}_i]$ $(i=1,2,...,N_k)$ such that $[0,k^{\mathrm{U}}]=\cup_{i=1}^{N_k}[\underline{k}_i,\overline{k}_i]$ and $[\underline{k}_i,\overline{k}_i]\cap[\underline{k}_l,\overline{k}_l]=\varnothing$, $\forall i\neq l$. Likewise, partition $[0,\omega^{\mathrm{U}}]$ into $[\underline{\omega}_j,\overline{\omega}_j]$ $(j=1,2,...,N_\omega)$. Then, the SHF representation for the 2D nonhomogeneous random wind field can be expressed as

$$u(z,t)=\sum_{i=1}^{N_k}\sum_{j=1}^{N_\omega}A(z,K_i,\Omega_j)\times[\cos(K_iz+\Omega_jt+\phi_{ij}^{(1)})+\cos(K_iz-\Omega_jt+\phi_{ij}^{(2)})] \quad (9)$$

where (K_i,Ω_j) is a random vector in the subdomain $D_{ij}=[\underline{k}_i,\overline{k}_i]\times[\underline{\omega}_j,\overline{\omega}_j]$ with the PDF $p_{K_i,\Omega_j}(k,\omega)$. $\phi_{ij}^{(1)}$'s and $\phi_{ij}^{(2)}$'s are uniform random phases independently distributed over [0,2π]. (K_i,Ω_j) is taken as a uniformly distributed random vector over D_{ij} as well, i.e., the PDF of (K_i,Ω_j) is

$$p_{K_i,\Omega_j}(k,\omega)=\frac{1}{(\overline{k}_i-\underline{k}_i)(\overline{\omega}_j-\underline{\omega}_j)} \quad (10)$$

It is easy to show that the correlation function of $u(z,t)$ is

$$
\begin{aligned}
&R_u(z,\xi,\tau)=E[u(z,t)u(z+\xi,t+\tau)]\\
&=\sum_{i=1}^{N_k}\sum_{j=1}^{N_\omega}E[A(z,K_i,\Omega_j)A(z+\xi,K_i,\Omega_j)\times\\
&\left(\frac{1}{2}\cos(K_i\xi+\Omega_j\tau)+\frac{1}{2}\cos(K_i\xi-\Omega_j\tau)\right)] \qquad (11)\\
&=\sum_{i=1}^{N_k}\sum_{j=1}^{N_\omega}\iint_{D_{ij}}A(z,K_i,\Omega_j)A(z+\xi,K_i,\Omega_j)\\
&\times\cos(K_i\xi)\cos(\Omega_j\tau)\,p_{K_i,\Omega_j}(k,\omega)\,\mathrm{d}\Omega_j\mathrm{d}K_i
\end{aligned}
$$

Meanwhile, similar to that in 1D nonstationary cases (Chen et al. 2017), the prescribed correlation function of $u(z,t)$ can be obtained from Wiener-Khintchine formula,

$$
\begin{aligned}
&R_u^0(z,\xi,\tau)\\
&=\int_{-\infty}^{\infty}\int_{-\infty}^{\infty}\sqrt{S(z,k,\omega)}\sqrt{S(z+\xi,k,\omega)}e^{\mathrm{i}(\omega\tau+k\xi)}\mathrm{d}\omega\mathrm{d}k\\
&=4\int_0^{\infty}\int_0^{\infty}\sqrt{S(z,k,\omega)}\sqrt{S(z+\xi,k,\omega)}\\
&\qquad\times\cos(\omega\tau)\cos(k\xi)\mathrm{d}\omega\mathrm{d}k \qquad (12)\\
&=4\sum_{i=1}^{N_k}\sum_{j=1}^{N_\omega}\iint_{D_{ij}}\sqrt{S(z,K_i,\Omega_j)}\sqrt{S(z+\xi,K_i,\Omega_j)}\\
&\qquad\times\cos(K_i\xi)\cos(\Omega_j\tau)\,\mathrm{d}\Omega_j\mathrm{d}K_i
\end{aligned}
$$

Comparing Eqs.(11) and (12) term to term yields

$$
\begin{aligned}
A(z,K_i,\Omega_j)&=\sqrt{\frac{4S(z,K_i,\Omega_j)}{p_{K_i,\Omega_j}(k,\omega)}}\\
&=\sqrt{4S(z,K_i,\Omega_j)(\bar{k}_i-\underline{k}_i)(\bar{\omega}_j-\underline{\omega}_j)}
\end{aligned}
\qquad (13)
$$

2.3. Determination of the subdomain D_{ij} and random vector (K_i,Ω_j)

As interpreted in subsection 2.2, the wavenumber and frequency ranges of interest are firstly partitioned into a number of N_k and N_ω intervals, respectively. Then, D_0 can be partitioned into a number of N_kN_ω subdomains $D_{ij}=[\underline{k}_i,\bar{k}_i]\times[\underline{\omega}_j,\bar{\omega}_j]$ by tensor products.

According to Chen et al. (2018a) and Song et al. (2018a), the wind speed PSD value in the range close to the origin is far greater than that in the range away from the origin. Therefore, the computational efforts can be reduced by taking denser wavenumber-frequency points in the range close to the origin Chen et al. (2018a). The idea is followed in the present paper and a new discretization scheme is suggested as follows instead of that in Chen et al. (2018a).

The non-uniform discretized wavenumbers and frequencies is determined, respectively, by

$$
\begin{cases}
\bar{k}_i=(k^{\mathrm{U}}/N_k)\times N_k^{(i/N_k)},(i=1,2,...,N_k)\\
\underline{k}_i=\bar{k}_{i-1},(i=2,3,...,N_k);\ \underline{k}_i=0,(i=1)
\end{cases}
\qquad (14)
$$

$$
\begin{cases}
\bar{\omega}_j=(\omega^{\mathrm{U}}/N_\omega)\times N_\omega^{(j/N_\omega)},(j=1,2,...,N_\omega)\\
\underline{\omega}_j=\bar{\omega}_{j-1},(j=2,3,...,N_\omega);\ \underline{\omega}_j=0,(j=1)
\end{cases}
\qquad (15)
$$

in this way, the lengths of the subintervals in wavenumber and frequency direction approximately exponentially increase as the subintervals depart away from the origin. An example of the partitioned subdomains obtained by tensor products after the operation of Eqs.(14) and (15) is shown in Figure 1.

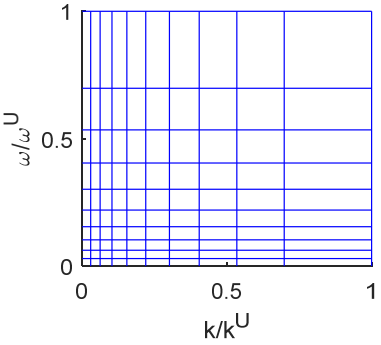

Figure 1: Example of partitioned subdomains obtained by the suggested scheme.

Since the subdomains have been specified, the random vector (K_i,Ω_j) is determined by

$$
\begin{cases}
K_i=\underline{k}_i+(\bar{k}_i-\underline{k}_i)\lambda_i^{(1)}\\
\Omega_j=\underline{\omega}_j+(\bar{\omega}_j-\underline{\omega}_j)\lambda_j^{(2)}
\end{cases}
\qquad (16)
$$

where $\lambda_i^{(1)}$'s and $\lambda_j^{(2)}$'s are uniform random variables independently distributed over [0,1]. In this way, the SHF representation for wind speed fields can be implemented conveniently based on Eqs.(14), (15) and (16).

3. NUMERICAL EXAMPLE

Consider a standard 5-MW offshore wind turbine model (Jonkman et al. 2009). Simulation of fluctuating wind speed field for the 90m high tower is carried out in this section.

Parameters of the joint spectrum are determined as follows: the decay coefficients is $C_z = 7$ (Peng et al. 2017), the average wind speed at the height of hub ($z = 90\text{m}$) is $U_{\text{ref}} = 20\text{m/s}$; the turbulence intensity is $I_{\text{ref}} = 0.16$; the standard deviation of turbulence is $\sigma_u = I_{\text{ref}} U_{\text{ref}} = 3.2\text{m/s}$. It is ready to obtain $\sigma_u^2 = 6u_*^2$ by integrating $S^{\text{Kai}}(z,\omega)$ with respect to ω, thus, $u_* = 1.306\text{m/s}$; z_0 and U_{10} are then specified by Eq.(3): $z_0 = 0.197\text{m}$, $U_{10} = 12.8\text{m/s}$. The other parameters for the numerical simulation are: the upper cut-off wavenumber and frequency are $k^{\text{U}} = 0.5\pi$ rad/m and $\omega^{\text{U}} = 4\pi$ rad/s (Chen et al. 2018a), respectively; the time history length of wind speeds is $T = 600\text{s}$, and the time step of the simulation is $\Delta t = 0.25\text{s}$. The number of the partitioned intervals in wavenumber and frequency directions is $N_k = N_\omega = 50$ in this case.

A population of 500 samples are generated by the proposed method. To evaluate the performance of the method, the fluctuating wind speed samples at the heights 10m, 50m and 90m are employed in reproducing the ensemble statistical properties, including the auto-PSD, cross-correlation function and coherence function. The fluctuating wind speed time histories of a wind field sample for the three points are shown in Figure 2.

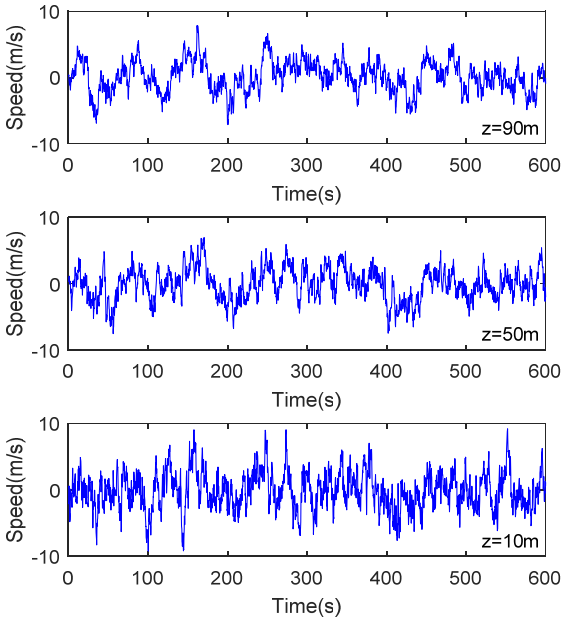

Figure 2: Fluctuating wind speed time histories at different heights.

Based on the simulated samples, the auto-PSD, the cross correlation function and the coherence function of the fluctuating wind speed processes can be estimated (Chen et al. 2018a). The comparisons between the reproduced values and the target values among the three points are shown in Figures 3-5, respectively.

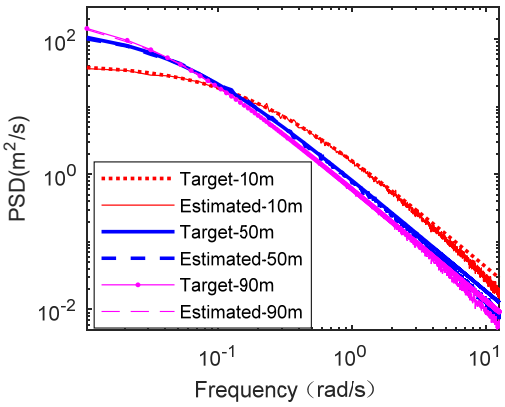

Figure 3: Comparisons of the estimated spectra with prescribed Kaimal spectrum at different heights.

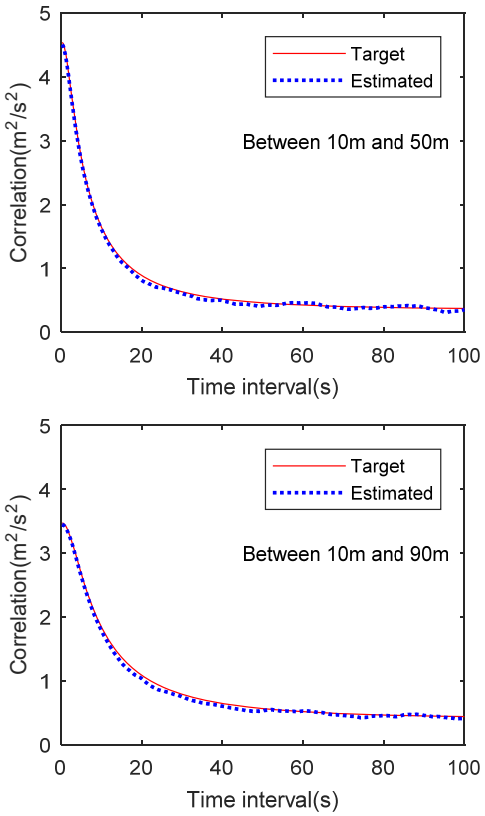

Figure 4: Comparisons between estimated and target cross-correlation functions between different heights.

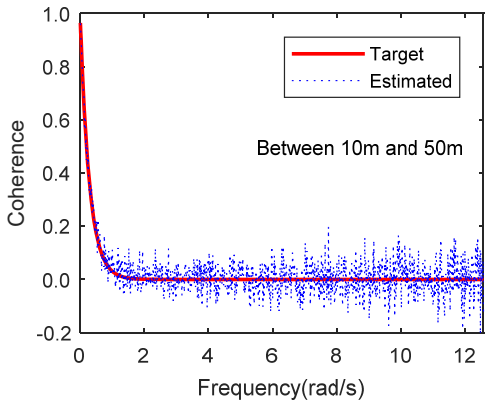

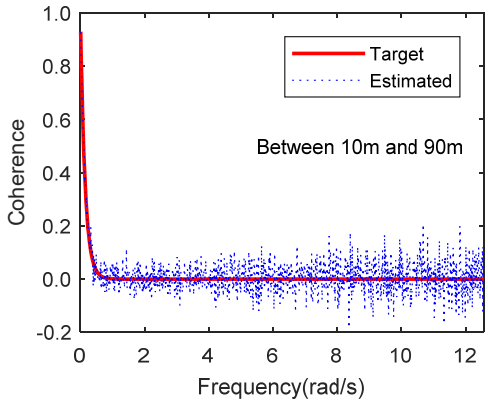

Figure 5: Comparisons between estimated and target coherence functions between different heights.

It is seen that the estimated values of the auto-PSD, the cross correlation function and the coherence function are well consistent with the target values, demonstrating the effectiveness of the proposed method. Besides, the number of the harmonic components involved in this case is only 2500, whereas, it is around 10^6 in the SRM. Therefore, the computational efforts and the number of random variables are greatly reduced.

4. CONCLUSIONS

The SHF representation has been extended to simulate nonhomogeneous wind speed random fields in one-spatial dimension based on the wavenumber-frequency joint spectrum. In this method, both the phase angles and frequencies (wavenumbers) are regarded as random variables. Particularly, the subdomains of wavenumber-frequency are determined by tensor products after the axes of wavenumber and frequency are non-uniformly discretized by exponential spaces approximately. The conclusions include: (1) The SHF representation for random fields can reproduce the target PSD exactly by a very finite number of harmonic components; (2) Compared to the SRM, the number of random variables and computational efforts in the SHF representation can be dramatically reduced in the simulation of wind speed fields. Meanwhile, the high accuracy is maintained.

The present paper focus on the simulation of fluctuating wind speed fields in one spatial

dimension. Simulation of fluctuating wind speed fields in two spatial dimensions is to be done in the future.

ACKNOWLEDGMENTS

Financial supports from the National Natural Science Foundation of China (Grant Nos. 51725804, 11672209, and 11761131014) and the International Joint Research Program of Shanghai Municipal Government (Grant No. 18160712800) are highly appreciated.

5. REFERENCES

Benowitz, B.A. and Deodatis, G. (2015). Simulation of wind velocities on long span structures: A novel stochastic wave based model. Journal of Wind Engineering & Industrial Aerodynamics, 147:154-163.

Chen, J.B., Song, Y.P., Peng, Y.B., et al. (2018a). Simulation of homogeneous fluctuating wind field in two spatial dimensions via a wavenumber-frequency joint power spectrum. Journal of Engineering Mechanics, 144(11): 04018100.

Chen, J.B., He, J.R., Ren, X.D., et al. (2018b). Stochastic harmonic function representation of random fields for material properties of structures. Journal of Engineering Mechanics, 144(7): 040118049.

Chen, J.B., Kong, F., Peng, Y.B. (2017). A stochastic harmonic function representation for non-stationary stochastic processes. Mechanical Systems & Signal Processing, 96: 31-44.

Chen, J.B., Sun, W.L., Li, J., et al. (2013). Stochastic harmonic function representation of stochastic processes. Journal of Applied Mechanics, 80(1): 011001.

Huang, M.F., Wang, Y.F., Lou, W.J., et al. (2018). Multi-scale simulation of time-varying wind fields for Hangzhou Jiubao Bridge during Typhoon Chan-hom. Journal of Wind Engineering & Industrial Aerodynamics, 2018, 179.

Li, J., Yan, Q., Chen, J.B. (2012). Stochastic modeling of engineering dynamic excitations for stochastic dynamics of structures, Probabilistic Engineering Mechanics. 27 (1): 19-28.

Liu, Z.J., Liu, Z.H., Peng, Y.B. (2018). Simulation of multivariate stationary stochastic processes using dimension-reduction representation methods. Journal of Sound and Vibration, 418: 144-162.

Peng, L.L., Huang, G.Q., Chen, X.Z., et al. (2017). Simulation of multivariate nonstationary random processes: hybrid stochastic wave and proper orthogonal decomposition approach. Journal of Engineering Mechanics, 143(9): 04017064.

Shinozuka, M. (1971). Simulation of multivariate and multidimensional random processes. Journal of the Acoustical Society of America, 49(1): 357-368.

Song, Y.P., Chen, J.B., Peng, Y.B., et al. (2018a). Simulation of nonhomogeneous fluctuating wind speed field in two-spatial dimensions via an evolutionary wavenumber-frequency joint power spectrum. Journal of Wind Engineering & Industrial Aerodynamics, 179: 250-259.

Song, Y.P., Chen, J.B., Peng, Y.B. (2018b). Simulation of nonhomogeneous fluctuating wind field in one-dimensional space by evolutionary wavenumber-frequency joint power spectrum. Engineering Mechanics, accepted. (in Chinese)

Spanos, P.D., Beer, M., Red-Horse, J. (2007). Karhunen–Loeve expansion of stochastic processes with a modified exponential covariance kernel, Journal of Engineering Mechanics, 133(7): 773–779.

Tao, T.Y., Wang, H., Kareem, A. (2018). Reduced-Hermite bifold-interpolation assisted schemes for the simulation of random wind field. Probabilistic Engineering Mechanics, https://doi.org/10.1016/j.probengmech.2018.08.002

Zeng, X.S., Peng, Y.B., Chen, J.B. (2017). Serviceability based damping optimization of randomly wind-excited high-rise buildings. The Structural Design of Tall and Special Buildings, e1371, doi: 10.1002/tal.1371.